



Interleukin-7 improves the fitness of regulatory T cells for adoptive transfer

Ilaria Cosorich¹ | Jessica Filoni¹ | Carla Di Dedda¹  | Arianna Ferrari¹ |
Tatiana Jofra¹ | Susanna Cesarano² | Chiara Bonini^{2,3} | Lorenzo Piemonti^{1,3} |
Paolo Monti¹ 

¹Transplant Immunology Lab, San Raffaele Diabetes Research Institute, IRCCS Ospedale San Raffaele Milan, Milan, Italy

²Experimental Hematology Unit, Division of Immunology, Transplantation and Infectious Diseases, Ospedale San Raffaele Scientific Institute, Milan, Italy

³Vita-Salute San Raffaele University, Milan, Italy

Correspondence

Paolo Monti, Transplant Immunology Lab, Diabetes Research Institute, IRCCS San Raffaele Scientific Institute, Via Olgettina 58, 20132 Milan, Italy.
Email: monti.paolo@hsr.it

Funding information

European Foundation for the Study of Diabetes; Fondazione Italiana Diabete; Juvenile Diabetes Research Foundation International, Grant/Award Number: 2-SRA-2021-1002-S-B; EFSD/JDRF/Lilly European Program in Type 1 Diabetes Research; Fondazione Italiana Diabete (FID)

Abstract

Adoptive regulatory T-cell (Treg) transfer has emerged as a promising therapeutic strategy for regulating immune responses in organ transplantation, graft versus host disease, and autoimmunity, including Type 1 diabetes. Traditionally, Treg for adoptive therapy have been sorted and expanded in vitro using high doses of IL-2, demonstrating stability and suppressive capabilities. However, limitations in their long-term survival post-infusion into patients have been observed. To address this challenge, we investigated a novel expansion protocol incorporating interleukin-7 (IL-7) alongside the traditional method utilizing IL-2 (referred to as IL-7 method, IL-7M). Our study revealed that naïve Treg express significant levels of CD127 and display robust responsiveness to IL-7, characterized by STAT-5 phosphorylation. Expanding naïve Treg with the IL-7M protocol led to a substantial enrichment of CD45RA⁺CD62L⁺CD95⁺ Treg but showing a reduction in the final cell yield and suppressive function. Moreover, Treg expanded with the IL-7M exhibited preserved telomere length and demonstrated enhanced resistance to cytokine withdrawal and fas-mediated apoptosis. When transferred into NSG mice IL-7M-Treg persisted longer and reduced the expansion of T cells, but did not significantly reduce the severity of xenoGvHD. In conclusion, our data demonstrate the feasibility of expanding naïve Treg in the presence of IL-7 to generate a Treg product enriched in poorly differentiated CD45RA⁺ cells with enhanced survival capabilities.

KEYWORDS

IL-7, immunometabolism, regulatory T cells

INTRODUCTION

CD4⁺CD25⁺FOXP3⁺ regulatory T cells (Treg) represent a T-cell subset specialized in the regulation of the immune response and maintenance of immune tolerance [1, 2].

These properties make Treg an appealing candidate for adoptive immunotherapy to control transplant rejection [3], graft versus host disease [4], and autoimmunity [5], including Type 1 diabetes (T1D) in more than 50 active or completed clinical trials [6]. Although polyclonal Treg remain

This is an open access article under the terms of the [Creative Commons Attribution-NonCommercial-NoDerivs](https://creativecommons.org/licenses/by-nc-nd/4.0/) License, which permits use and distribution in any medium, provided the original work is properly cited, the use is non-commercial and no modifications or adaptations are made.

© 2023 The Authors. *Immunology* published by John Wiley & Sons Ltd.

the most commonly used in the clinical setting, chimeric antigen receptor (CAR) or T cell receptor (TCR) transgenic Treg are expected to become widely available in the near future [7]. In current adoptive immunotherapy protocols Treg are isolated from peripheral blood and expanded in vitro to yield a therapeutically valuable Treg product with stability and suppressive function. However, the “first-in-man” clinical trial with polyclonal Treg in T1D patients revealed some limitations in terms of long-term survival of the adoptively transferred Treg [8]. Specifically, it showed a bi-phasic exponential decay kinetic with a short-lived Treg subset (75%–90%) exhibiting a half-life of few days, and a long-lived Treg subset (10%–25%) detectable up to 1 year after infusion. Interestingly, the surviving Treg displayed a CCR7⁺CD45RA⁺CD45RO^{-/+} phenotype similar to less differentiated naïve or memory stem T cells. Conventionally, Treg are isolated as CD4⁺CD25^{high}CD127^{low} [9] and expanded using anti CD3/CD38 microbeads in combination with high doses IL-2, a potent mitogen and pro-differentiating cytokine that promotes memory subsets generation [10]. Alternatively, homeostatic cytokines such as IL-7 and IL-15 can support T-cell expansion while preserving a poorly differentiated phenotype. Studies conducted on conventional T cells showed the capacity of IL-7 [7] or combination of IL-7 and IL-15 [11] to generate memory stem T cells from naïve precursors after expansion. Despite low expression of the IL-7Ralpha (CD127) [9] human naïve Treg have been shown to respond to and proliferate in the presence of IL-7 in vitro [12]. Furthermore, in conditions of Treg depletion, IL-7 contributes to Treg compartment reconstitution in patients treated with the anti-CD25 monoclonal antibody basiliximab [13].

To investigate the hypothesis that modifying the in vitro expansion protocol to promote Treg expansion while maintaining a poorly differentiated CD45RA⁺ phenotype may enhance Treg resistance to stress signals and improve long-term survival following infusion in adoptive transfer protocols, we sorted Treg (CD4⁺CD25^{high}CD127^{low}) exhibiting a naïve CD62L⁺CD45RA⁺CD95⁻ phenotype and included IL-7 in the culture medium during expansion. Our findings suggest that expansion in the presence of IL-7 generates a Treg product with an immature phenotype and improved resistance to stress and apoptosis.

RESULTS

Responsiveness to IL-7 in circulating naïve and memory Treg subsets

As for conventional T cells, also circulating Treg can be categorized according to surface phenotypes corresponding to

naïve or memory subsets. According to the expression of CD45RA, CD62L, and CD95, we determined the relative proportion (%: median, interquartile range [IQR]) of Treg naïve (10.1, 7–16.3 Treg-n; CD45RA⁺CD62L⁺CD95⁻), Treg stem cells memory (1.2, 0.6–2.6 Treg-scm, CD45RA⁺CD62L⁺CD95⁺), Treg central-memory (44.8: 32.5–59.6 Treg-cm, CD45RA⁻CD62L⁺CD95⁺), Treg effector-memory (42.5, 35.8–52.1 Treg-em, CD45RA⁻CD62L⁻CD95⁺) and Treg effector-memory re-expressing CD45RA (0.4, 0.2–0.6 Treg-emra, CD45RA⁺CD62L⁻CD95⁺) in peripheral blood samples from 16 adult healthy subjects (Figure 1a,b). In parallel, we determined the relative proportion of circulating conventional CD4⁺ T cells in the same subjects (Supplementary Figure 1A,B). Using this phenotypic classification, we detected all the subsets described for conventional T cells, including Treg with a Tscm phenotype that have never been described before. As Treg are characterized by a low expression of CD127 [14], we measured (median fluorescence intensity [MFI]; median, IQR) the expression of CD127 in all the Treg subsets identified and compared it to the one of conventional bulk CD4⁺ T cells (3205, 2064–4692) and CD19⁺ B cells (57, 49–69) that do not express CD127 [15] (Figure 1c). Treg-n showed the brightest expression of CD127 (480, 316–611) followed by Treg-scm (432; 304–515), Treg-cm (328; 246–390), Treg-em (173, 122–236), and Temra (132, 101–159). Subsequently, STAT-5 phosphorylation was measured after incubation Treg with IL-7 (10 ng/mL for 1 min) to assess whether the functional status of CD127 and its expression STAT5 are sufficient to elicit intracellular signalling (Figure 1d). We compared STAT-5 phosphorylation (MFI; median, IQR) to the one of conventional CD4⁺ T cells (8056, 6730–10 526) and CD127⁻ B cells (167, 126–168). Treg-n showed the strongest STAT-5 phosphorylation (3386, 2794–4629) followed by Treg-scm (2540, 1972–2817), Treg-cm (1500, 950–1827), Treg-em (779, 364–909), Treg-emra (576, 332–776). These data show that Treg were responsive to IL-7, especially those with a naïve or stem cell memory phenotype, even though their responsiveness to IL-7 was lower than the one of conventional CD4⁺ T cells. Subsequently, we conducted comparative analysis of Treg expansion in response to IL-2, IL-7 or their combination (Figure 1e). Treg displayed a restricted fold expansion (median, IQR) in response to IL-7 [8–11], whereas they exhibited robust expansion in the presence of IL-2 (85, 68–95). Surprisingly, the combination of IL-7 and IL-2 induced an intermediate level of Treg expansion (54, 34–61) which was unexpectedly lower than that achieved with IL-2 alone. Our interpretation of these findings suggests a competition between IL-2 and IL-7 for the common gamma chain, resulting in an intermediate proliferation rate rather than an additive or synergistic effect. This hypothesis is supported by our

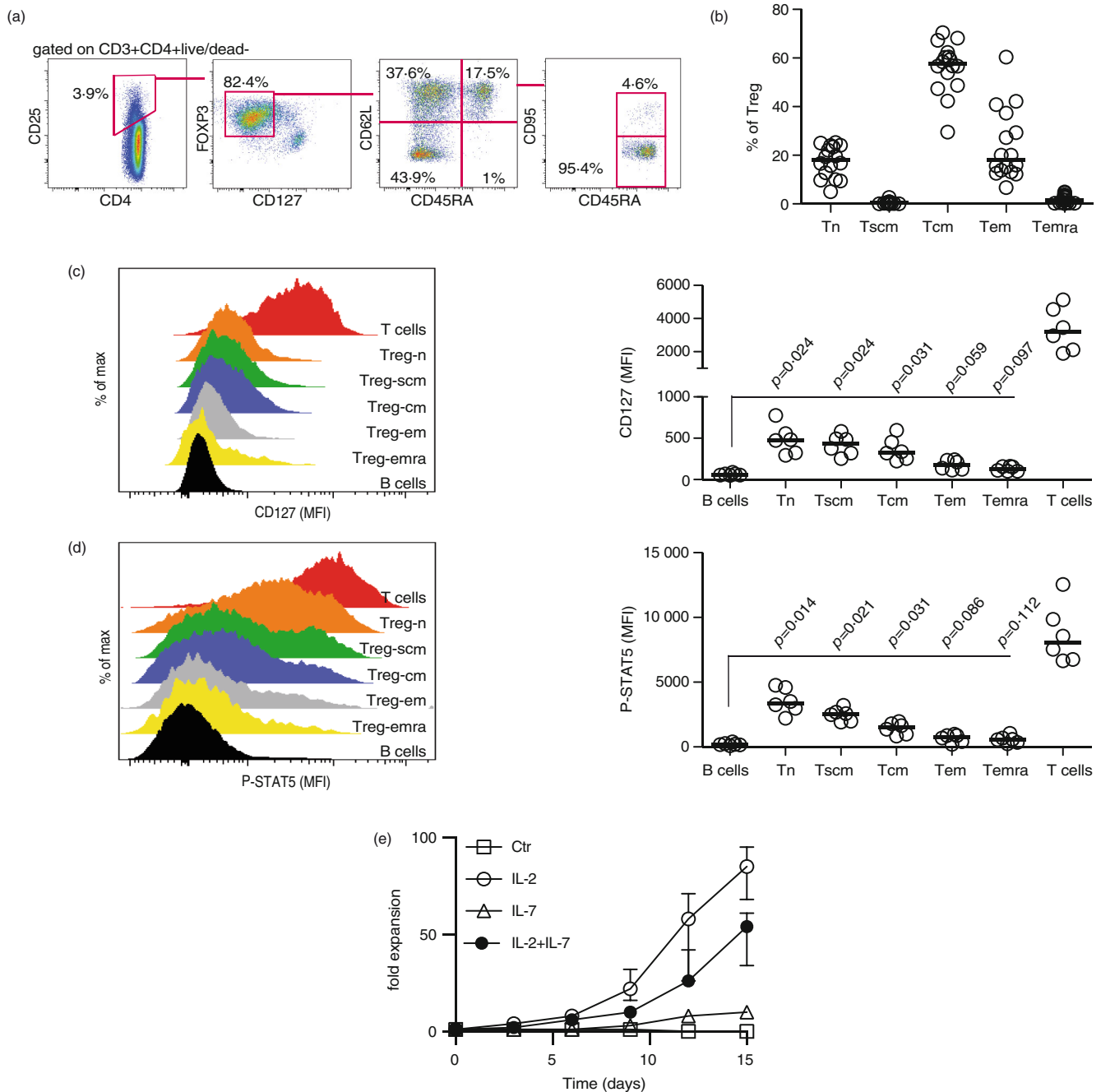


FIGURE 1 Responsiveness to IL-7 of circulating Treg subsets. (a) Representative FACS plots showing the gating strategy to identify Treg (CD4⁺CD25^{high}FOXP3⁺CD127^{low}) and naïve and memory subsets based on the expression of CD62L, CD45RA, and CD95. (b) Graph shows percentage of each of Treg subset from 16 subjects (c) Representative FACS plot (left) showing the expression of CD127 in Treg subsets compared to conventional CD4⁺ T cells and B cells, and graph representing data from six subjects (right). (d) Representative FACS plot (left) showing STAT-5 phosphorylation in Treg subsets compared to conventional CD4⁺ T cells and B cells after 10 min incubation with 10 ng/mL of rh-IL-7 (left) measurements from six subjects (right). (e) Expansion curve of bulk Treg cultured with medium (Ctr), IL-2 (100 UI/mL), IL-7 (10 ng/mL), and combination of IL-2 and IL-7 ($n = 3$). IL-7, interleukin-7.

previous research, where we demonstrated that blocking the IL-2 receptor alpha with a monoclonal antibody increased the availability of the common gamma chain, rendering conventional T cells more responsive to IL-7

[16]. To gain deeper insights into this competition mechanism, we conducted experiments to determine the binding of IL-2 FITC in the presence of IL-7 as well as the binding of IL-7 FITC in the presence of IL-2. The

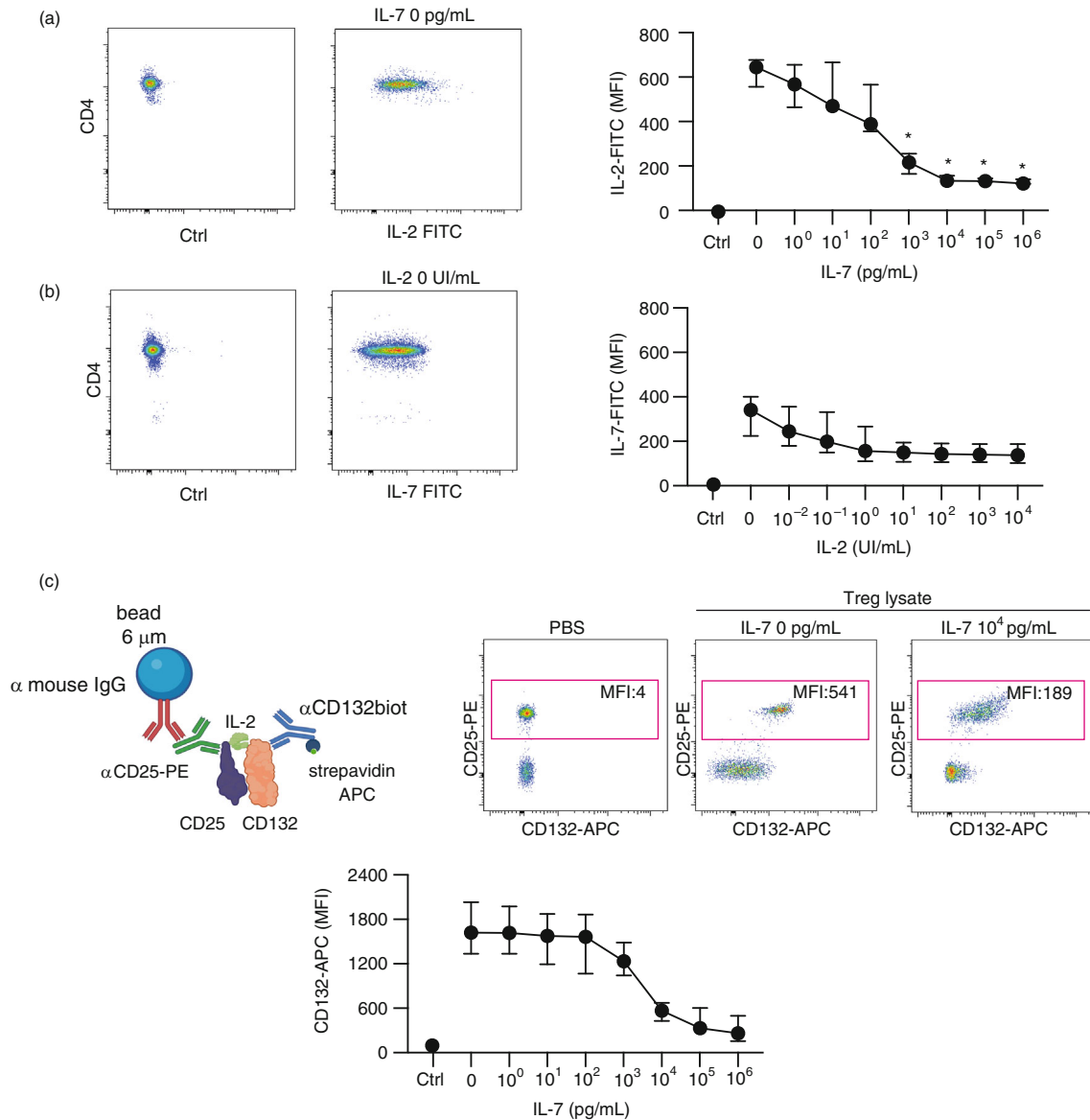


FIGURE 2 IL-2 receptor and IL-7 receptor competition. (a) FACS plot showing the binding of IL-2-FITC (or unlabelled IL-2) to the Treg cell surface in the absence of IL-7 (left). The graph displays the binding of IL-2-FITC in the presence of increasing concentrations of IL-7 (0–10⁶ pg/mL) (right). (b) FACS plots showing the binding of IL-7-FITC (or unlabelled IL-7) to the Treg surface in the absence of IL-2 (left). The graph illustrates the binding of IL-7-FITC in the presence of increasing concentrations of IL-2 (0–10⁴ UI/mL) (right). (c) Flow cytometric assay to measure the association of CD25 and CD132 using beads. CD127 was linked to anti-mouse IgG1-coupled beads through a mouse-IgG1-anti-CD25 PE complex. CD132 association was determined by a biotinylated anti-CD132 and streptavidin APC. FACS plots shows the fluorescence of CD132 APC on beads alone (left), beads incubated with cell lysate from Treg incubated in PBS (centre), and beads incubated with 10⁴ pg/mL of IL-7. The graph demonstrates the fluorescence of CD132 APC on beads incubated with increasing concentrations of IL-7 (0–10⁶ pg/mL). IL-2, interleukin-2; IL-7, interleukin-7.

results revealed a progressive decrease in the binding of IL-2 to Treg with increasing concentrations of IL-7, with a reduction of 70% in the presence of 10⁴ pg/mL of IL-7 (Figure 2a). Conversely, the impact of IL-2 on the binding of IL-7 FITC to Treg was less pronounced, resulting in a reduction of 45% at 100 UI of IL-2 (Figure 2b). To formally demonstrate the interference of

IL-7 with the association of CD25 and CD132 (and possibly CD122) to form the high affinity IL-2 receptor, we developed a co-precipitation assay (Figure 2c) similar to the one we have previously shown [16]. Treg, pre-treated with increasing concentrations of IL-7, exhibited a progressive reduction in the association of the CD25/CD132 complex, suggesting that IL-7 limited the

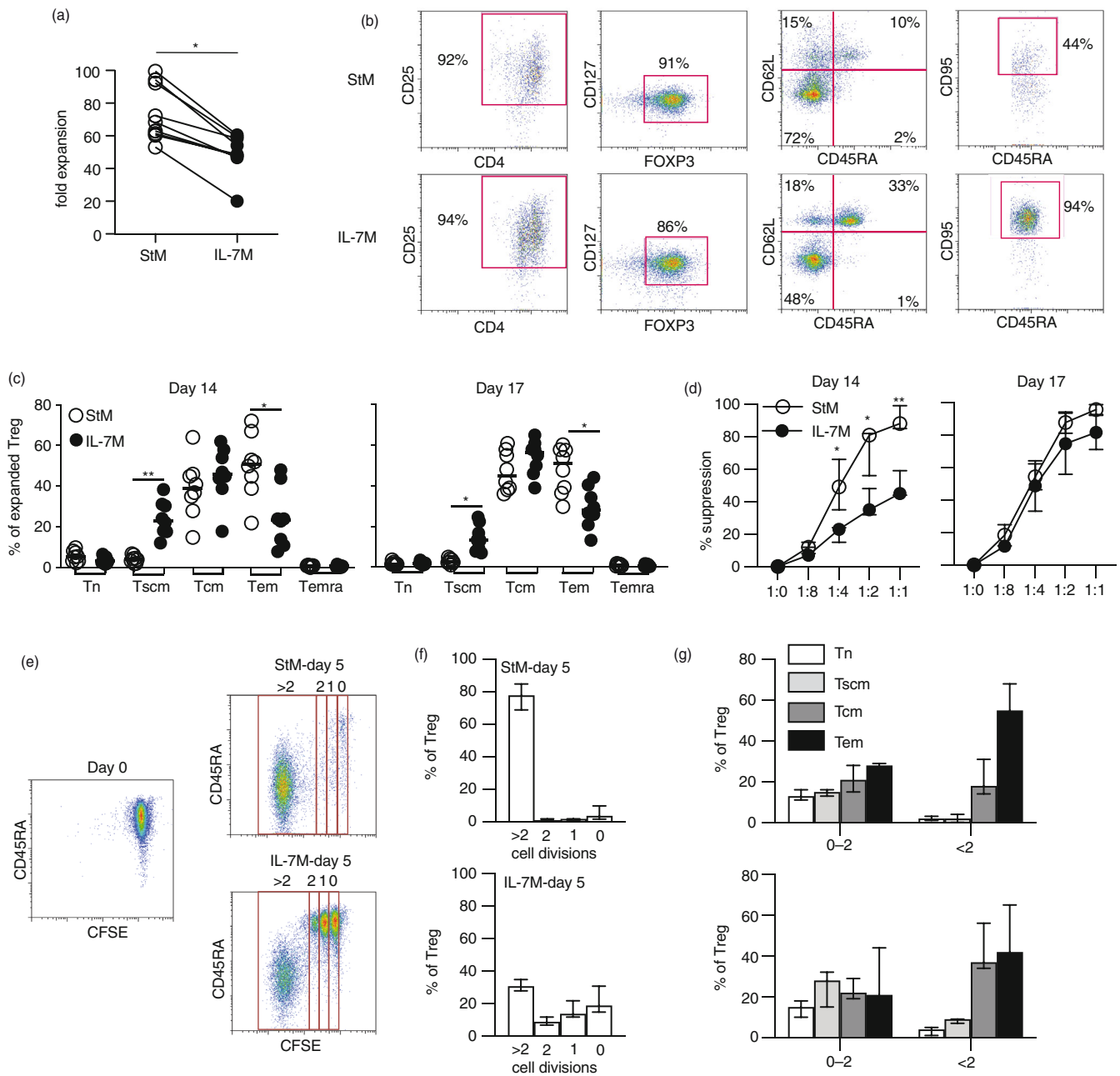


FIGURE 3 Expansion of Treg in the presence of IL-7. (a) Fold expansion of naïve Treg after 14 days culture with the StM (aCD3CD28 beads + 100UI/mL rh IL-2) and the IL-7M (aCD3CD28 beads + 100UI/mL rh IL-2 + 10 ng/mL rhIL-7; $n = 9$ individual donors). (b) Representative FACS plots showing the phenotype of StM-Treg or IL-7M-Treg after expansion. (c) Graph shows the percentage Treg subsets in StM-Treg or IL-7M-Treg after 14 days expansion, at Day 17 after resting (medium only; $n = 8$). (d) Suppression assay using StM-Treg or IL-7M-Treg after 14 days of expansion, and at Day 17 after resting (medium only; $n = 3$). (e) CFSE dilution assay showing the number of cell cycles performed by StM-Treg or IL-7M-Treg in the first 5 days of expansion. (f) Graph shows the percentage of cells in each cycle after 5 days. (g) Graph shows the percentage of cells displaying T naïve (Tn, CD45RA⁺CD62L⁺CD95⁻), T stem cell memory (Tscm, CD45RA⁺CD62L⁺CD95⁺), T central memory (Tcm, CD45RA⁻CD62L⁺CD95⁻), T-effector memory (tem, CD45RA⁻CD62L⁻CD95⁺) phenotype. IL-7, interleukin-7; StM, standard method.

availability of CD132 required to form the high affinity IL-2 receptor complex. These findings collectively indicate the possibility to expand Treg using a combination of IL-7 and IL-2, with the subset displaying a naïve and

stem cell memory phenotype showing the strongest responsiveness to IL-7. Based on these results, we decided to expand sorted CD45RA⁺CD62L⁺ Treg in the presence of IL-7 and IL-2.

Expansion, phenotype, and suppressive capacity of naïve Treg expanded with IL-2 (StM-Treg) or a combination of IL-2 and IL-7 (IL-7M-Treg)

We conducted a comparative study of two methods for expansion of highly purified (Supplementary Figure 2A–C) sorted CD45RA⁺CD62L⁺ Treg (Treg-n/Treg-scm). The standard method (StM: anti CD3/CD28 microbeads at 1:1 ratio in the presence of 100UI of rhIL-2) was compared to the IL-7 method (IL-7M) similar to the StM but with the addition of 10 ng/mL of rhIL-7. After 14 days of expansion, StM-Treg exhibited greater expansion (fold expansion: 68, 61–93) than IL-7M-Treg (fold expansion: 49, 47–59, $p = 0.021$), resulting in a 28% decrease in the final cell yield of IL-7M-Treg (Figure 3a). Surface phenotype analysis revealed that IL-7M-Treg were highly enriched in CD45RA⁺CD62L⁺CD95⁺ cells (Figure 3b). When dividing Treg into subsets according to the expression of CD45RA, CD62L, and CD95, we observed that both StM-Treg and IL-7M-Treg displayed similar percentages (median, IQR) of Treg-n (StM 5.4, 3.4–8.1 vs. IL-7M 3.5, 2.4–5.5, $p = 0.234$), Treg-cm (StM 39, 29.7–45.7 vs. IL-7M 46, 40.1–57, $p = 0.458$) and Treg-emra (StM 1.1, 0.8–1.2 vs. IL-7M 1, 0.3–1.2, $p = 0.88$) after 14 days of expansion (Figure 3c). Notably, IL-7M-Treg exhibited a significant enrichment in Treg-scm (StM 4.3, 2.6–6 vs. IL-7M 23.2, 17.9–31, $p = 0.0078$) and a lower abundance Treg-em (StM 51, 40.5–63.5 vs. IL-7M 23.5, 11.7–39, $p = 0.0375$; Figure 3c). Following the 14-day expansion, Treg cultures underwent magnetic depletion of anti CD3/CD28 microbeads and were further cultured for additional 3 days without cytokines for a resting period. Post-resting, both StM-Treg and IL-7M-Treg demonstrated preservation of the relative percentages of Treg subsets. Subsequently we conducted suppression assays against CD8⁺ T cells, showing a significant reduction in the suppressive activity of IL-7M-Treg compared to StM-Treg (Figure 3d). Since we have shown that IL-7 can reduce the Treg suppressive activity but the suppressive function is re-established once IL-7 is removed [12], we tested Treg after a 3-day resting period, which resulted in a full recovery of the suppressive function after removal of IL-7. To determine whether the kinetic of proliferation can impact on the differences in the phenotype of expanded Treg we analysed the phenotype of proliferating Treg according the dilution of carboxyfluorescein succinimidyl ester (CFSE) after 5 days of expansion. StM-Treg exhibited a homogeneous proliferation pattern, with the majority undergoing multiple cell cycles and losing the expression of CD45RA (Figure 3e,f). Conversely, IL-7M-Treg can be classified in two groups: one performing multiple cell cycles and losing CD45RA, and a second

group undergoing a limited number of cell cycles while preserving CD45RA expression. Notably, sorted Treg that underwent more than two cell cycles in both StM-Treg and the IL-7M-Treg predominantly differentiated into Treg-cm and Treg-em (Figure 3g). Conversely, sorted Treg undergoing fewer than two cell cycles predominantly differentiated into Treg-n and Treg-scm. These findings suggest that a population of slowly proliferating cells, that is predominant within IL-7M-Treg, but very scarce in StM-Treg, accounts for the abundance of cells exhibiting a stem cell memory phenotype in the final Treg product after 14 days of culture. Collectively, these data suggest that the presence of IL-7 reduces the proliferation rate (and the final cell yield), while maintaining a less differentiated phenotype. Moreover, the diminished suppressive function can be restored after a brief culture in the absence of IL-7.

In vitro performances of StM-Treg and IL-7M-Treg

Given the rapid and significant reduction of expanded Treg once infused in patients, we sought to assess the in vitro performance of StM-Treg and IL-7M-Treg. First, we focused on parameters associated with bioenergetic metabolism that could influence the metabolic fitness of expanded Treg. In vitro expansion of Treg commonly occurs under high glucose concentrations and oxygen availability. However, these conditions may not always be met in the human body, where glucose concentration is 5.5 mM or below and oxygen availability varies depending on the anatomical location. This could potentially impact the ability of infused Treg to fulfil their metabolic needs. IL-7M-Treg exhibited an increased mitochondrial mass (MFI, IQR) compared to StM-Treg (StM-Treg 422, 240–743 vs. IL-7M-Treg 1221, 1082–1427, $p = 0.031$). This was measured using the MitoTracker™ Green dye, which accumulates in mitochondria regardless of mitochondrial membrane potential (Figure 4a). However, the mitochondrial membrane potential ($\Delta\psi$ M), measured using the MitoTracker® Deep Red FM dye, showed no significant differences between the two groups (Figure 4b). To assess glucose uptake capacity, we performed a dynamic assay, measuring the uptake of the glucose analogue 2-(N-(7-nitrobenz-2-oxa-,1,3-diazol-4-yl) amino)-2-deoxyglucose (2NBDG) over a 50-min time window. The data were analysed by comparing the differences in the area under the curve (AUC). IL7M-Treg exhibited a greater capacity to accumulate 2NBDG compared to StM-Treg (AUC; StM-Treg 3.5×10^6 vs. IL-7M-Treg 4.8×10^6) (Figure 4c). In addition, IL-7M-Treg produced more lactate than StM-Treg (StM 182, 133–233

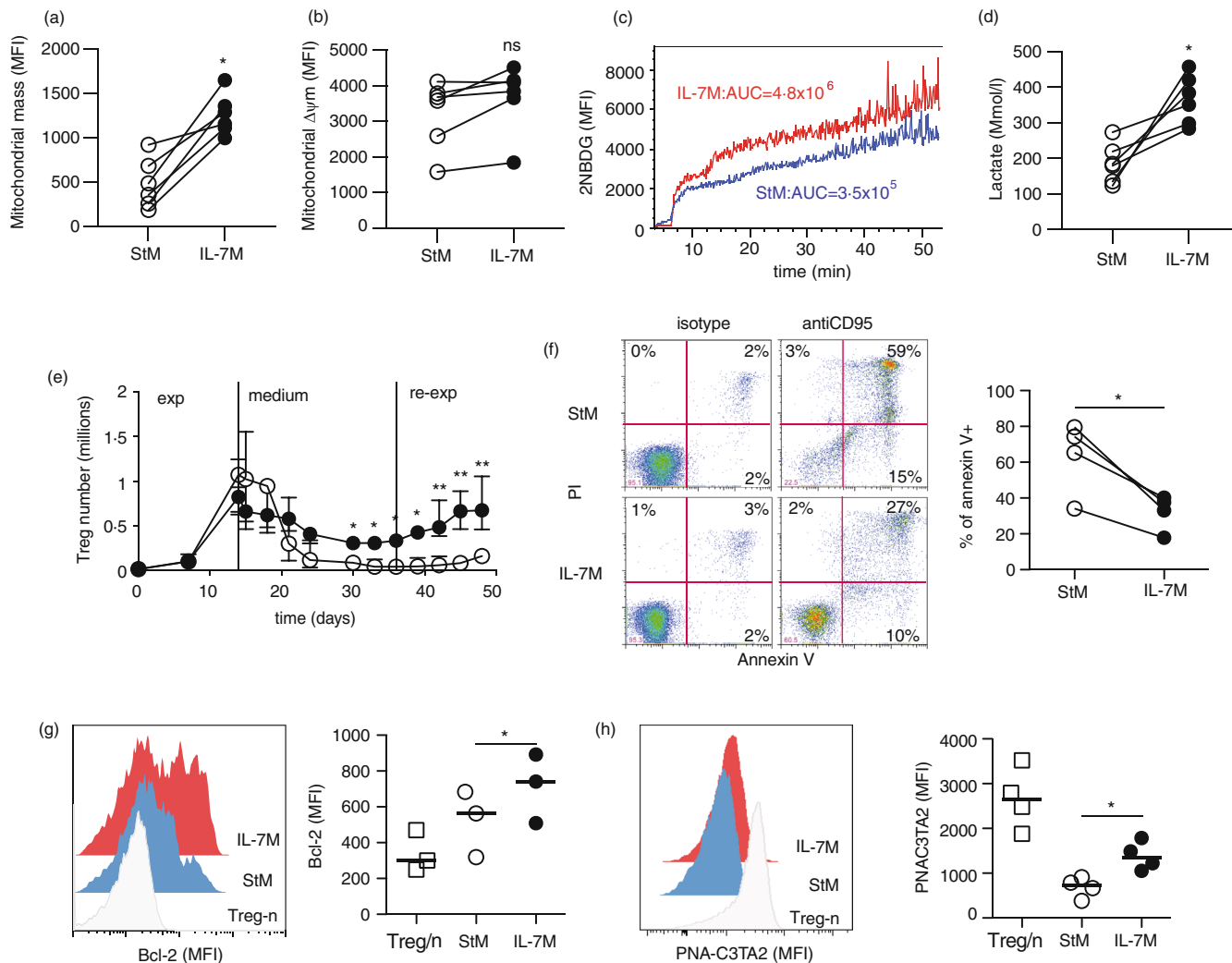


FIGURE 4 Bio-energetic profile, apoptosis and telomere length of Treg expanded in the presence of IL-7. (a) Mitochondrial mass, (b) mitochondrial $\Delta\psi_m$, (c) dynamic measurement of 2NBDG uptake, and (d) lactate concentration (mmol/L) in the supernatant of StM-Treg or IL-7M-Treg. (e) StM-Treg or IL-7M-Treg were cultured for 3 weeks in medium without aCD3/CD28 beads or cytokines. The absolute number of live cell is reported in the graph. After 3 weeks, remaining Treg were re-stimulated with aCD3/CD28 beads and 100 UI rhIL-2. (f) Representative FACS plot (left) of annexin V and propidium iodide staining in expanded StM-Treg or IL-7M-Treg and cultured with an agonistic anti-fas monoclonal antibody for 24 h. Graph representing four independent experiments is shown on the right. (g) Representative FACS plot (left) showing Bcl-2 expression StM-Treg or IL-7M-Treg compared to freshly isolated naïve Treg ($n = 3$). (h) Telomere length was measured by flow cytometry using a PNAC₃TA₂ probe in StM-Treg or IL-7M-Treg compared to freshly isolated naïve Treg ($n = 4$). IL-7, interleukin-7; StM, standard method; 2NBDG, 2-(N-(7-nitrobenz-2-oxa-,1,3-diazol-4-yl)amino)-2-deoxyglucose.

vs. IL-7M 367, 295–430, $p = 0.03$; Figure 4d), suggesting an increased glycolytic rate. These immuno-metabolic signatures were preserved after a three-day resting period albeit with reduced intensity (Supplementary Figure 3A). To assess the performance of Treg under stress conditions, we conducted experiments where expanded Treg were cultured without cytokines and antiCD3/CD28 microbeads. Interestingly, the number of IL-7M-Treg declined at a slower rate compared to StM-Treg. After 2 weeks of culture a significantly higher number IL-7M-Treg was still

viable (absolute number $\times 10^3$; StM-Treg: 46, 26–71 vs. IL-7M-Treg 338, 272–386, $p = 0.031$) (Figure 4e). Moreover, when cytokines and beads were reintroduced to the culture, IL-7M-Treg displayed the ability to re-expand after a second challenge. To further test Treg resilience after 14 days of expansion, we tested a direct pro-apoptotic stimulus by adding an agonistic anti-fas IgM antibody for 12 h. The percentage of cells undergoing apoptosis was significantly lower in IL-7M-Treg (% annexin V⁺: StM 69.8, 41.9–78.2 vs. IL-7M, 35.4, 21.6–39.6, $p = 0.018$;

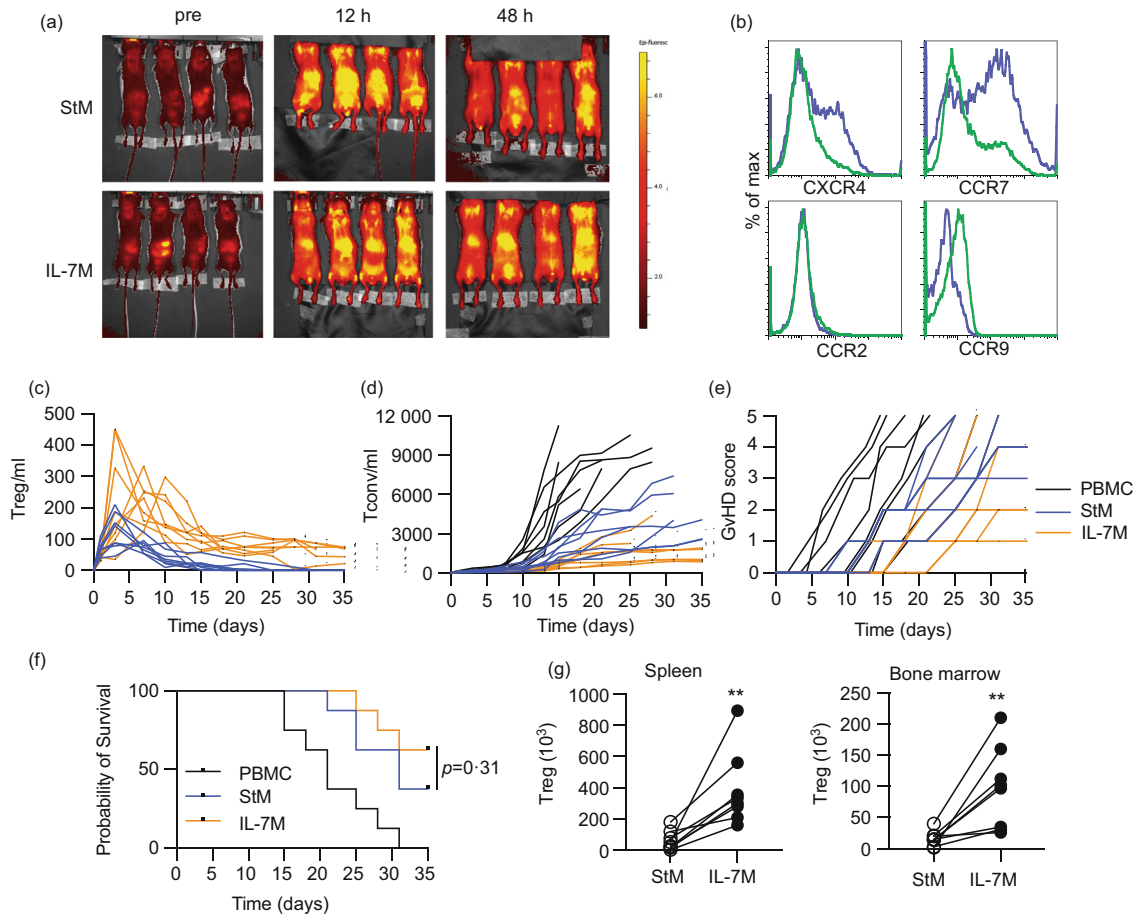


FIGURE 5 Homing and survival of Treg in NSG mice. (a) IVIS images of NSG mice injected with StM-Treg or IL-7M-Treg at time 0 (pre-injection), 12 h and 48 h after Treg injections. (b) FACS plots showing the expression of CXCR4, CCR7, CCR2, and CCR9 on StM-Treg (green line) or IL-7M-Treg (blue line). (c) NSG mice were infused with PBMC either alone or in combination with StM-Treg or IL-7M-Treg. Graph shows circulating StM-Tregs or IL-7M-Treg (Treg/mL) over time for each individual NSG mouse. (d) Graph shows circulating T cells (Tcells/mL) over time for each individual NSG mouse. (e) GvHD score calculated over time for each individual NSG mouse. (f) Kaplan-Meier survival curve comparing NSG mice receiving human PBMC alone or in combination with expanded StM-Tregs or IL-7M-Treg (eight animals for each group). (g) Absolute number of Treg (Treg/mL) in the spleen and bone marrow of NSG mice after sacrifice. IL-7, interleukin-7; StM, standard method.

Figure 4f). As IL-7 was shown to up-regulate the anti-apoptotic molecule Bcl-2, we measured Bcl-2 in both StM-Treg and IL-7M-Treg and compared to non-expanded Treg-n (Figure 4g). Both StM-Treg and IL-7M-Treg displayed an upregulation of Bcl-2 compared to the non-expanded Treg-n. However, IL-7M-Treg displayed a significantly higher expression of Bcl-2 compared to StM-Treg (MFI: StM-Treg 464, 320–684 vs. IL-7M-Treg 892, 510–1142, $p = 0.043$). Finally, we measured the length of telomeric DNA after expansion as telomere erosion is associated with cell senescence. Both StM-Treg and IL-7M-Treg displayed a substantial reduction in telomere length compared to non-expanded Treg-n. However, IL-7M-Treg exhibited a significant preservation of telomeric DNA compared to StM-Treg (MFI: StM-Treg 729, 456–880 vs. IL-7M-Treg 1356, 1095–1712, $p = 0.0158$).

Homing, survival and protection from xeno GvHD of StM-Treg and IL-7M-Treg in NSG mice

To determine differences in the in vivo homing capacity and survival, VivoTrack-680 labelled StM-Treg or IL-7M-Treg were injected in the tail vein of NSG mice and monitored for 48 h using the in vivo imaging systems (IVIS) technology. After injection of StM-Treg, we observed an increased signal in the bladder (Figure 5a). As the labelling dye is excreted with urine we interpreted this signal as a consequence of increased cell death and release of free dye that accumulate in the bladder. After injection of IL-7M-Treg we noticed an increased signal in the femurs of mice, indicating an improved home capacity to the bone marrow. Corroborating these findings, we observed

an increased expression of CXCR4 in Treg expanded with the IL-7M (Figure 5b). Treg expanded with the IL-7M showed also an increased expression of CCR7 (also in line with a poorly differentiated phenotype), a similar but very low expression of CCR2 and a reduced expression of CCR9, indicating other possible differences in the migratory pattern of StM-Treg and IL-7M-Treg.

To compare survival and protection from xenoGvHD of Tregs expanded with the StM or their inhibitory function *in vivo*, we used a xenograft model of lethal GvHD [17]. IL-7M-Treg survived longer than StM-Treg ($p = 0.0131$; Figure 5c) and better controlled the expansion of conventional T cells ($p = 0.012$; Figure 5d). However, longer persistence of IL-7M-Treg was not associated with a significant reduction of GvHD symptoms (GvHD score calculation in Supplementary Figure 4A; $p = 0.078$; Figure 5e) or to a significant improvement of survival ($p = 0.31$; Figure 5f). Corroborating the findings of increased survival capacity IL-7M-Treg were more abundant in the spleen and bone marrow of mice after sacrifice (Figure 5g).

DISCUSSION

Adoptive transfer of Treg holds therapeutic promise in controlling immune responses and restoring peripheral tolerance in transplantation, GVHD, and autoimmune diseases. In a future perspective, TCR-engineered, or CAR Treg are anticipated to rapidly emerge as alternative options to polyclonal Treg. However, the clinical experience has revealed certain challenges that may affect the therapeutic efficacy of this approach. Specifically, the requirement for a large number of Treg for adoptive therapy has been met with robust *in vitro* expansion protocols. Nevertheless, the expanded Treg have displayed vulnerabilities and a limited capacity to persist in patients. In addition, identifying measurable biological parameters beyond just cell yield is essential to predict the expanded Treg's capacity to adapt to the *in vivo* environment, characterized by competition with other cells for growth factors and nutrients, leading to selective pressure.

In this study, we demonstrate that Treg can be effectively expanded using a combination of IL-7 and IL-2, offering several advantages in terms of resistance to apoptosis and stress as well as the preservation of a poorly differentiated phenotype. These findings are significant for improving Treg expansion protocols in adoptive Treg therapy and addressing issues related to the long-term persistence of Treg infused in patients.

The *in vitro* expansion of Treg for adoptive transfer has traditionally relied on high doses of IL-2 [18–20].

This results in a final Treg product comprising mainly short-lived Treg *in vivo*, alongside a long-lived subset capable of persisting for more than a year [8]. Based on studies primarily focused on conventional T cell, we proposed the use of homeostatic cytokines for Treg expansion. Among these, IL-7 induces conventional T-cell expansion [21] and provides anti-apoptotic signals [22]. Despite Treg having low expression of the IL-7 receptor alpha chain, leading to the assumption that they do not respond to IL-7, we explored its potential in Treg expansion. Treg are phenotypically defined as $CD4^+CD25^{\text{high}}FOXP3^+$ T cells and sorted as $CD4^+CD25^{\text{high}}CD127^{\text{low}}$ T cells for *in vitro* expansion [14]. Interestingly, unlike circulating B cells lacking CD127 [15] we observed a low but significant expression of CD127 in Treg, sufficient to trigger significant STAT5 phosphorylation upon IL-7 stimulation at 10 ng/mL. Our previous findings indicated that Treg are responsive to IL-7, although at higher concentrations compared to conventional T cells [12]. Under physiological IL-7 concentrations of 2–8 pg/mL [23], Treg are less likely to receive significant signals. However, during *in vitro* expansion when IL-7 is used at high concentration, a robust response to IL-7 is elicited. Notably, we also reported that in patients experiencing lymphopenia, where IL-7 is present at supra-physiological concentrations, it contributes to Treg homeostasis and proliferation, thus reconstituting the depleted Treg compartment [13]. The responsiveness to IL-7 was more pronounced in Treg exhibiting a naïve or memory stem T-cell phenotype and diminished as differentiation progressed into central-memory and effector-memory subsets. Importantly, the responsiveness was not solely related to changes in CD127 expression, suggesting the involvement of other unidentified factors regulating STAT-5 phosphorylation. This heightened IL-7 responsiveness of $CD45RA^+CD62L^+$ Treg was a key reason for our decision to sort $CD45RA^+CD62L^+$ for expansion. In addition, we aimed to obtain a Treg product with an immature phenotype, as these cells appear to survive longer in patients [8]. To trigger significant Treg expansion we combined IL-7 with IL-2. Surprisingly, this combination did not yield an additive or synergistic effect; instead, the presence of IL-7 led to a reduction in the proliferation rate induced by IL-2. We experimentally proved that in the presence of IL-7, the formation of the high-affinity IL-7 receptor engaged a substantial amount of the common- γ chain (CD132), consequently reducing the ability of IL-2 to form the high-affinity IL-2 receptor with CD25, CD122, and CD132. We have previously demonstrated a competition of CD127 and CD25 for CD132 in conventional T cells [16]. As a result of this competition, expansion of $CD45RA^+CD62L^+$ Treg with the IL-7M resulted in a

reduced final cell yield, along with a distinctive surface phenotype where a significantly higher proportion of Treg display a CD45RA⁺CD62L⁺CD95⁺ phenotype. This phenotype is reminiscent of conventional memory stem T cells [24] and, to the best of our knowledge, Treg with a stem cell memory phenotype have not been described before. Further investigations are necessary to clarify whether such a subset with memory stem cell function exist within the Treg compartment, displaying characteristics of self-renewal and the capacity to generate the full phenotypic diversity of Treg subsets. In addition, expanded Treg from cord blood exhibited increased CD95 expression compared to expanded Treg from peripheral blood [25], which also contain a higher proportion of CD45RA⁺CD62L⁺ Treg. This phenotypically immature Treg population obtained with the IL-7M also demonstrated relevant differences in terms of metabolic machinery and survival capacity. The improved metabolic fitness, including enhanced mitochondrial mass and glucose uptake, could confer an advantage to IL-7M-Treg once infused into patients. Notably, Treg cells are less reliant on glycolysis, favouring mitochondrial metabolism and oxidative phosphorylation (OXPHOS) for energy production compared to conventional T cells [26]. In vitro studies have highlighted the direct role of Foxp3 in reprogramming T-cell metabolism by suppressing glycolysis and enhancing OXPHOS [27, 28]. Although elevated glycolysis can be detrimental to Treg induction and suppressive function, the deletion of HIF-1a, a transcription factor promoting glycolysis, results in increased Foxp3 induction [29]. Nevertheless, Treg still require glycolysis to support certain processes like proliferation [30] and migration [31] when a high amount of ATP and metabolic intermediates are needed. It is reasonable to speculate that Treg cells precisely balance cellular glucose consumption, utilizing glycolysis to increase proliferation and expansion, while relying on OXPHOS to maintain lineage stability and suppressive activity. In our study, IL-7M-Treg showed signs of increased glycolysis (as evidenced by 2NBDG uptake and lactate production) along with an increased mitochondrial mass. Interestingly, a reduction of glycolysis after a few days of resting corresponded to a recovery of the Treg suppressive capacity. Importantly, Treg adoptive transfer involves moving Treg from in vitro culture conditions, characterized by high glucose, oxygen and intense cytokine and TCR/CD28 signalling, to an in vivo environment where these factors are reduced or of unknown composition. Hence, an improved metabolic machinery may help Treg in adapting to changing conditions and surviving in vivo overcoming substrate and growth factor signalling limitations. Our study also revealed an increased survival capacity of IL-7M-Treg both after growth factor deprivation and in response to direct apoptotic stimuli.

This enhanced resistance to fas ligand-mediated apoptosis in IL-7M-expanded Treg could be attributed to the increased expression of the anti-apoptotic molecule Bcl-2, presumably induced by the presence of IL-7 [22]. In addition, we observed a reduced telomere shortening in IL-7M-Treg. Telomere length is regulated by telomere erosion during cell division, and by the activity of telomerase, which is negligible in T cells [32]. Preserving telomere length during IL-7-mediated T-cell expansion has been reported [32], and in our Treg expansion model, this could also be due to the reduced rate of expansion of IL-7M-Treg. Preliminary data indicate an increased capacity of IL-7M-Treg to survive in NSG mice as well as a distribution pattern that includes migration to the bone marrow. While increased persistence of IL-7M-Treg was observed alongside a reduction of conventional T-cell expansion, the severity of GvHD and the survival of mice did not reach statistical significance. This can be attributed to the reduced suppressive capacity of IL-7M-Treg, indicating the need for further studies to enhance the suppressive function.

In conclusion, while IL-7-mediated Treg expansion shows promise in terms of increased persistence, further investigations are necessary to optimize their suppressive function. By refining our approach, we aim to advance the field of adoptive Treg therapy and overcome the challenges posed by the fragility of these cells, ultimately maximizing the therapeutic benefits of this promising immunotherapy.

METHODS

Cell isolation, purification, and FACS analyses

Sodium-heparinized peripheral venous blood samples were kindly provided by the Immunohematology and Transfusion Medicine Service of San Raffaele hospital, Milan, Italy and were derived from healthy donors who donate blood. Highly purified (98%) naive Treg were isolated using the FACS Aria II according to the expression of CD4-PB (Clone SK3), CD25-APC-Cy7 clone (eBioDDR5), CD127-PE-CY7 (clone HIL-7R-M21), CD45RA-PE-Cy5 (clone HI-100), CD62L-PE (clone DREG-56), and CD95-APC (clone DX2) all from BD Biosciences (Supplemental Figure 1). The same antibodies were used for FACS analysis and with the additional staining for FOXP3-AF488 (clone PCH101, from eBioscience). According to the experimental needs STAT5 phosphorylation was measured using anti STAT5 pY694 Alexa Fluor 647 (clone 47, BD Biosciences) and Bcl-2 was detected using anti Bcl-2 APC (clone Bcl-2/100, BD Biosciences). Telomere length was measured using a

fluorescein conjugated PNA probe kit from DAKO. Apoptosis was measured using an annexin V-propidium iodide staining kit from BD Biosciences.

IL-7 and IL-2 binding to receptors and association of CD25 and CD132

IL-7 and IL-2 binding to their respective receptors on the cell surface were measured using the IL-7 or the IL-2 Fluorokine kit according to manufacturer instructions (R&D System). Tregs were suspended in PBS at 4×10^6 cells/mL in the presence of rhIL-2 (Bio-Techne) or rhIL-7 (R&D Systems) at concentrations as indicated in Figure 2 for 15 min at 37°C and incubated 1 µg/mL of biotinylated IL-7 or IL-2 for 20 min on ice. Avidin-FITC was then added for an additional 30 min. Finally, cells were washed in PBS and analysed by FACS. To determine the association of IL-2 with CD25 and CD132 Treg were suspended in X-vivo 15 without serum and incubated with or without IL-7 at concentrations indicated in Figure 2 for 15 min at 37°C. Treg were washed twice in PBS and cell pellets were frozen at -80°C , subsequently thawed and lysed in 50 mM Hepes, 150 mM NaCl, 15 mM MgCl_2 , 1 mM EDTA, 10% glycerol, and 1% Triton X-100. For the detection of association of CD25 and CD132, cell lysates were incubated with anti-CD25 PE (mouse IgG1, clone M-A251) on ice for 20 min. Anti-mouse IgG1,j-coupled beads (Comp beads, BD-Pharmingen) or uncoupled beads as control were added to the lysates for 20 min on ice to bind the anti-CD25 complex to the beads. Association of CD132 with CD25 was detected after washing beads in PBS containing bovine serum albumine and incubation with biotinylated anti-CD132 (rat IgG2j, clone TUGh4) for 20 min on ice. Beads were then incubated with streptavidin-APC for 20 min at room temperature, washed and analysed by flow cytometry.

In vitro expansion protocols

Sorted naïve Treg were plated at 5×10^4 /mL in 96-well U bottom plate (Costar) with X-VIVO 15 medium (Lonza, catalogue no. 04-418Q) containing 5% heat-inactivated pooled bovine serum (Sigma-Aldrich). In the StM culture medium was supplemented with Dynabeads human T-activator CD3/CD28 (Thermofisher) at a 1:1 bead/cell ratio, and 100 UI/mL rhIL-2 (Bio-Techne). In the IL-7 method (IL-7M), culture medium of the StM was supplemented also with rhIL-7 (R&D Systems) at 10 ng/mL. Treg were cultured for 14 days and the culture medium and supplements were replaced at Days 7 and 11.

Treg homing and persistence and GvHD in NSG mice

Homing of Treg was evaluated using the IVIS technology. Treg expanded with StM or the IL-7M were labelled with VivoTrack-680 (Perkin Elmer) and 2×10^6 of labelled cells were injected intravenously into NSG mice. In vivo monitoring of labelled cells was done in a Lumina II IVIS imaging system (Caliper Life Science), by recording fluorescence at an excitation wavelength of 675 nm and emission 582 filter of 690–770 nm. Data analysis was done using the Living Image software v. 4.2 (Caliper Life Sciences). To determine persistence of Treg in NSG mice, 1×10^6 GFP⁺StM-Treg or GFP⁺IL-7M-Treg were injected in NSG mice along with 10^7 autologous peripheral blood mononuclear cells (PBMC). Blood samples were collected to detect the presence of Treg or conventional T cells. GvHD score was calculated according to the score shown in Supplemental Figure 4A.

Suppression assay

After expansion Treg were stained with eFluor 670 Cell Proliferation Dye and co-cultured with CFSE-stained, FACS-sorted, allogenic CD8⁺ T cells at 1:1, 1:2, 1:4, 1:8, and 1:0 T cell:Treg ratios in the presence of anti CD3/CD28 beads at 1:10 cell/bead ratio. Cell culture was harvested at Day 5 and the percentage of proliferating (CFSE-diluted) T cells was calculated. The percentage of suppression was calculated as $100 - [100 \times (\text{percentage of proliferating cells with Treg present})/(\text{percentage of proliferating cells without Treg present})]$.

T-cell bio-energetic profile

Surrogate markers of oxidative phosphorylation and glycolysis were measured by flow cytometry using the following reagents according to the manufacturer's instructions. MitoTracker Green FM and MitoTracker Red FM were from Invitrogen-Molecular Probes. 2NBDG was from Life Technologies. L(+)lactate concentration was measured in the supernatants with a Lactate Assay Kit (Sigma-Aldrich).

Statistical analysis

Statistical analyses were performed using GraphPad Prism software. Flow cytometry data were calculated as MFI and subpopulations as percentage of positive cells. Proliferation was calculated as percentage of cells that diluted the fluorescent dye CFSE (%CFSEdim). Data were

presented as median and IQR, and the Wilcoxon matched-pairs test was used for comparisons. A two-tailed *p*-value of 0.05 was considered significant.

Study approval

Blood donors signed an informed consent in accordance with the D.M., 2 November 2015, entitled 'Provisions relating to the quality and safety requirements of blood components'. In accordance with the ministerial provisions and the IOG 364 institutional procedure 'Request and delivery of buffy coats for research purposes', it is not possible to retrieve any type of information (gender, age, human leukocyte antigens typing) of donors. The animal study protocol was approved by the local animal ethics committee of San Raffaele Hospital (IACUC n 532/2022-PR, approved 12 September 2022).

AUTHOR CONTRIBUTIONS

Ilaria Cosorich, Jessica Filoni, Arianna Ferrari, Tatiana Jofra, Susanna Cesarano, and Carla Di Dedda designed and performed the experiments, analysed data, and contributed to write the paper. Lorenzo Piemonti, Chiara Bonini, and Paolo Monti designed the study, supervised the work, analysed data, and wrote the paper. Paolo Monti is the guarantor of this work and, as such, had full access to all the data in the study and takes responsibility for the integrity of the data and the accuracy of the data analysis.

ACKNOWLEDGEMENT

Open access funding provided by BIBLIOSAN.

FUNDING INFORMATION

This study was supported by a EFSD/JDRF/Lilly European Program in Type 1 Diabetes Research, by a grant from Fondazione Italiana Diabete (FID), and the Juvenile Diabetes Research Foundation, JDRF (2-SRA-2021-1002-S-B).



CONFLICT OF INTEREST STATEMENT

The authors declare no conflict of interest.

DATA AVAILABILITY STATEMENT

The data that support the findings of this study are available from the corresponding author upon reasonable request.

ORCID

Carla Di Dedda  <https://orcid.org/0000-0002-7472-8681>
 Paolo Monti  <https://orcid.org/0000-0002-4452-2164>

REFERENCES

1. Sakaguchi S, Yamaguchi T, Nomura T, Ono M. Regulatory T cells and immune tolerance. *Cell*. 2008;133(5):775–87.
2. Plitas G, Rudensky AY. Regulatory T cells: differentiation and function. *Cancer Immunol Res*. 2016;4(9):721–5.
3. Atif M, Conti F, Gorochoy G, Oo YH, Miyara M. Regulatory T cells in solid organ transplantation. *Clin Transl Immunol*. 2020;9(2):1–15.
4. Guo WW, Su XH, Wang MY, Han MZ, Feng XM, Jiang EL. Regulatory T cells in GVHD therapy. *Front Immunol*. 2021;12:12.
5. Esensten JH, Muller YD, Bluestone JA, Tang Q. Regulatory T-cell therapy for autoimmune and autoinflammatory diseases: the next frontier. *J Allergy Clin Immunol*. 2018;142(6):1710–8.
6. Raffin C, Vo LT, Bluestone JA. T reg cell-based therapies: challenges and perspectives. *Nat Rev Immunol*. 2021;20(3):158–72.
7. Mohseni YR, Tung SL, Dudreuilh C, Lechler RI, Fruhwirth GO, Lombardi G. The future of regulatory T cell therapy: promises and challenges of implementing CAR technology. *Front Immunol*. 2020;11:1–13.
8. Bluestone JA, Buckner JH, Fitch M, Gitelman SE, Gupta S, Hellerstein MK, et al. Type 1 diabetes immunotherapy using polyclonal regulatory T cells. *Sci Transl Med*. 2015;7(315):315ra189.
9. Seddiki N, Santner-Nanan B, Martinson J, Zaunders J, Sasson S, Landay A, et al. Expression of interleukin (IL)-2 and IL-7 receptors discriminates between human regulatory and activated T cells. *J Exp Med*. 2006;203(7):1693–700.
10. Hoffmann P, Eder R, Kunz-Schughart LA, Andreesen R, Edinger M. Large-scale in vitro expansion of polyclonal human CD4⁺CD25⁺ high regulatory T cells. *Blood*. 2004;104(3):895–903.
11. Vignali D, Cantarelli E, Bordignon C, Canu A, Citro A, Annoni A, et al. Detection and characterization of CD8⁺ autoreactive memory stem T cells in patients with type 1 diabetes. *Diabetes*. 2018;67:936–45.
12. Heninger A-K, Theil A, Wilhelm C, Petzold C, Huebel N, Kretschmer K, et al. IL-7 abrogates suppressive activity of human CD4⁺CD25⁺FOXP3⁺ regulatory T cells and allows expansion of alloreactive and autoreactive T cells. *J Immunol*. 2012;189(12):5649–58.
13. Vignali D, Gürth CM, Pellegrini S, Sordi V, Sizzano F, Piemonti L, et al. IL-7 mediated homeostatic expansion of human CD4⁺CD25⁺FOXP3⁺ regulatory T cells after depletion with anti-CD25 monoclonal antibody. *Transplantation*. 2016;100(9):1853–61.
14. Liu W, Putnam AL, Xu-yu Z, Szot GL, Lee MR, Zhu S, et al. CD127 expression inversely correlates with FoxP3 and suppressive function of human CD4⁺ T reg cells. *J Exp Med*. 2006;203(7):1701–11.
15. Ryan DH, Nuccie BL, Ritterman I, Liesveld JL, Abboud CN, Insel RA. Expression of interleukin-7 receptor by lineage-negative human bone marrow progenitors with enhanced lymphoid proliferative potential and B-lineage differentiation capacity. *Blood*. 1997;89(3):929–40.
16. Monti P, Brigatti C, Heninger AK, Scirpoli M, Bonifacio E. Disengaging the IL-2 receptor with daclizumab enhances IL-7-



- mediated proliferation of CD4⁺ and CD8⁺ T cells. *Am J Transplant*. 2009;9(12):2727–35.
17. Chakraborty R, Mahendravada A, Perna SK, Rooney CM, Heslop HE, Vera JF, et al. Robust and cost effective expansion of human regulatory T cells highly functional in a xenograft model of graft-versus-host disease. *Haematologica*. 2013; 98(4):533–7.
 18. Battaglia M, Stabilini A, Roncarolo MG. Rapamycin selectively expands CD4⁺CD25⁺FoxP3⁺ regulatory T cells. *Blood*. 2005; 105(12):4743–8.
 19. Putnam AL, Brusko TM, Lee MR, Liu W, Szot GL, Ghosh T, et al. Expansion of human regulatory T-cells from patients with type 1 diabetes. *Diabetes*. 2009;58(3):652–62.
 20. MacDonald KN, Piret JM, Levings MK. Methods to manufacture regulatory T cells for cell therapy. *Clin Exp Immunol*. 2019;197(1):52–63.
 21. Tan JT, Dudl E, LeRoy E, Murray R, Sprent J, Weinberg KI, et al. IL-7 is critical for homeostatic proliferation and survival of naïve T cells. *Proc Natl Acad Sci U S A*. 2001;98(15):8732–7.
 22. Chetoui N, Boisvert M, Gendron S, Aoudjit F. Interleukin-7 promotes the survival of human CD4⁺ effector/memory T cells by up-regulating Bcl-2 proteins and activating the JAK/STAT signalling pathway. *Immunology*. 2010;130(3):418–26.
 23. Carrett F, Surh CD. IL-7 signaling and CD127 receptor regulation in the control of T cell homeostasis. *Semin Immunol*. 2012;24(3):209–17.
 24. Gattinoni L, Lugli E, Ji Y, Pos Z, Paulos CM, Quigley MF, et al. A human memory T cell subset with stem cell-like properties. *Nat Med*. 2011;17(10):1290–7.
 25. Motwani K, Peters LD, Vliegen WH, el-sayed AG, Seay HR, Lopez MC, et al. Human regulatory T cells from umbilical cord blood display increased repertoire diversity and lineage stability relative to adult peripheral blood. *Front Immunol*. 2020;11: 1–17.
 26. Procaccini C, de Rosa V, Galgani M, Abanni L, Cali G, Porcellini A, et al. An oscillatory switch in mTOR kinase activity sets regulatory T cell responsiveness. *Immunity*. 2010;33(6): 929–41.
 27. Angelin A, Gil-de-Gómez L, Dahiya S, Jiao J, Guo L, Levine MH, et al. Foxp3 reprograms T cell metabolism to function in low-glucose, high-lactate environments. *Cell Metab*. 2017;25(6):1282–1293.e7.
 28. Garriets VA, Kishton RJ, Johnson MO, Cohen S, Siska PJ, Nichols AG, et al. Foxp3 and toll-like receptor signaling balance Treg cell anabolic metabolism for suppression. *Nat Immunol*. 2016;17(12):1459–66.
 29. Shi LZ, Wang R, Huang G, Vogel P, Neale G, Green DR, et al. HIF1 α -dependent glycolytic pathway orchestrates a metabolic checkpoint for the differentiation of TH17 and Treg cells. *J Exp Med*. 2011;208(7):1367–76.
 30. Pacella I, Procaccini C, Focaccetti C, Miacci S, Timperi E, Faicchia D, et al. Fatty acid metabolism complements glycolysis in th selective regulatory t cell expansion during tumor growth. *Proc Natl Acad Sci USA*. 2018;115(28):E6546–55.
 31. Kishore M, Cheung KCP, Fu H, Bonacina F, Wang G, Coe D, et al. Regulatory T cell migration is dependent on glucokinase-mediated glycolysis. *Immunity*. 2017;47(5):875–89.
 32. Patrick MS, Cheng NL, Kim J, An J, Dong F, Yang Q, et al. Human T cell differentiation negatively regulates telomerase expression resulting in reduced activation-induced proliferation and survival. *Front Immunol*. 2019;10:1–11.

SUPPORTING INFORMATION

Additional supporting information can be found online in the Supporting Information section at the end of this article.

How to cite this article: Cosorich I, Filoni J, Di Dedda C, Ferrari A, Jofra T, Cesarano S, et al. Interleukin-7 improves the fitness of regulatory T cells for adoptive transfer. *Immunology*. 2023; 170(4):540–52. <https://doi.org/10.1111/imm.13690>